

Optical investigation of the electronic structure of single ultrathin InAs layers grown pseudomorphically on (100) and (311)A GaAs substrates

Maria-Isabel Alonso

Institut de Ciència de Materials de Barcelona, Consejo Superior de Investigaciones Científicas, 08193 Bellaterra, Spain, and Max-Planck-Institut für Festkörperforschung, Heisenbergstrasse 1, 70569 Stuttgart, Germany

Matthias Ilg

Max-Planck-Institut für Festkörperforschung, Heisenbergstrasse 1, 70569 Stuttgart, Germany

Klaus H. Ploog

Paul-Drude-Institut für Festkörperelektronik, Hausvogteiplatz 5-7, 10117 Berlin, Germany

(Received 18 November 1993)

We investigate the electronic structure of a series of InAs-monolayer and submonolayer structures synthesized on both (100) and (311)A GaAs substrates by molecular-beam epitaxy. The chosen growth conditions ensure excellent structural and optical quality of the samples. Consequently, we have the opportunity to analyze the electronic properties of these ultrathin InAs layers which we explore by high-resolution x-ray-diffraction, photoluminescence (PL) and PL excitation (PLE) measurements. InAs submonolayer structures with an InAs coverage down to $0.78 \times 10^{14} \text{ cm}^{-2}$ give characteristic x-ray-interference spectra that evolve continuously with increasing In content. In contrast, the optical spectroscopies reveal a clear crossover from electronically disconnected InAs clusters to quantum-well behavior at an InAs coverage of about $3 \times 10^{14} \text{ cm}^{-2}$ for both orientations studied. The energies of the features observed in PL and PLE spectra of these structures are modeled as a function of InAs layer thickness using an eight-band $\mathbf{k} \cdot \mathbf{p}$ -type effective-mass theory. The valence-band anisotropy of the bulk compounds is reflected in differences between both growth directions. In addition, our results indicate that the band offset ratio at the strained InAs/GaAs interface is orientation dependent.

I. INTRODUCTION

During the last years the strained epitaxial system (Ga,In)As/GaAs has gained the status of a model system for the study of strained semiconductor heterostructures. The demonstration of surfactant action in III-V semiconductor epitaxy was first carried out in this system.¹ Strain, as a parameter^{2,3} to tune the electronic band structure, has been studied in this system and exploited for numerous optoelectronic applications. Besides that, (Ga,In)As/GaAs quantum wells allow the study of fundamental aspects which are not accessible with the paramount (Al,Ga)As/GaAs model system. For instance, the excitonic binding energy turnover occurring in the regime of very thin quantum wells could be seen in the (Ga,In)As/GaAs system.⁴ The InAs/GaAs system, as the extreme representative of the (Ga,In)As/GaAs family, extends greatly the concept of ultrathin quantum wells. In addition, this system has potential for interesting device applications, either as an alternative to $\text{Ga}_x\text{In}_{1-x}\text{As}$ alloys,⁵ or in heterostructures in which monolayer or submonolayer InAs planes are inserted.⁶ As a result, a number of studies have focused on the topic of InAs quantum wells in a GaAs matrix.⁷⁻¹³

In this study, we present data on a series of (100)- and

(311)-oriented single InAs layers with InAs thicknesses ranging from 0.4 Å to 3.2 Å. The systematic study of the dependence of their optical properties on InAs thickness and growth direction allows us to investigate two open questions: Down to which InAs thickness can we use quantum-well models for the description of these structures? The work of Noda *et al.*⁶ gives data of an electrical measurement on a (100) sample with a 1.6-Å-thick InAs layer. However, up to now there exists neither a systematic nor an optical study of this issue. What is the orientation dependence of the electronic structure at a coherently strained interface? The previous quantitative study by Meléndez *et al.*¹³ was based on a single (311) sample which was severely affected by In segregation.

We describe the work in three main parts: First we show high-resolution double-crystal x-ray diffraction (HRDXD) data. Next, we present the results of the optical measurements. These measurements draw a borderline between samples with quantum-well characteristics and samples where the InAs sheet is built up by electronically disconnected clusters. Finally, we focus on the electronic transition energies which are modeled by using an eight-band $\mathbf{k} \cdot \mathbf{p}$ envelope-function calculation. Further, our results point to a dependence on orientation of the conduction-band offset at the strained InAs/GaAs interface.

II. EXPERIMENTAL DETAILS

We have investigated a series of heterostructures grown simultaneously on (100) and (311)*A* semi-insulating GaAs substrates by solid-source molecular-beam epitaxy. All samples consisted of one GaAs buffer layer of 1 μm thickness, followed by one single strained InAs monolayer or submonolayer, and a GaAs cap approximately 180 nm thick. Reflection high-energy electron diffraction (RHEED) was used to monitor the growth process *in situ*. The RHEED patterns observed for both orientations indicated a two-dimensional growth behavior. To achieve minimum In segregation, As-rich conditions and appropriate modulation of substrate temperature were chosen. This procedure has been shown¹⁴ to give high quality samples from a structural as well as an optical point of view, while no reevaporation of In is detected.

The strain state and precise In content within the InAs layers were characterized by HRDXD using a double-crystal x-ray diffractometer in Bragg geometry.¹⁵ A rotating-anode 12-kW generator with a copper target was employed as x-ray source, and an asymmetrically cut Ge(100) crystal served as monochromator and collimator. Two x-ray interference patterns were recorded for each sample in the vicinity of both a symmetric and an asymmetric reflection. For (100)-oriented samples these were the (400) and (422) reflections, and for (311) samples, the (311) and the (400) reflections, respectively. From simulation of the measured curves using the dynamical theory of x-ray diffraction we obtained the amounts of In quoted in the first column of Tables I and II as equivalent InAs layer thicknesses d_{InAs} . The data indicated that the layers are pseudomorphic in all cases. The measured In contents are close to those expected from measured growth rate of bulk InAs and the beam equivalent pressures before growth. Note that the quality of the fits is not altered by accepting slightly segregated In distributions while keeping the layers pseudomorphic. Hence, the technique of x-ray interferences is very precise in the determination of the total amount of In present in the sample, but it is not very sensitive to its actual distribution profile.

TABLE I. Experimental parameters of the investigated samples grown in (100) orientation, as obtained from x-ray diffraction and optical spectroscopies: Average thickness of the InAs layer, energy and FWHM of the PL emission, and energies of the two observed interband transitions.

d_{InAs} (\AA)	E_{PL} (eV)	FWHM (meV)	$E_{e\text{-hh}}$ (eV)	$E_{e\text{-lh}}$ (eV)
0.4				
1.1	1.508	3.0		
1.5	1.496	7.1 ^a		
2.0	1.484	4.1	1.488	1.507
2.2	1.482	4.9	1.488	1.504
3.0	1.445	8.4	1.445	1.490
3.2	1.441	8.0	1.451	1.488
3.7	1.409	25.0

^aComposed peak.

TABLE II. Experimental parameters of the investigated samples grown in (311) orientation, as obtained from x-ray diffraction and optical spectroscopies: Average thickness of the InAs layer, energy and FWHM of the PL emission, and energies of the two observed interband transitions.

d_{InAs} (\AA)	E_{PL} (eV)	FWHM (meV)	$E_{e\text{-hh}}$ (eV)	$E_{e\text{-lh}}$ (eV)
0.4				
0.9	1.506	2.0		
1.5	1.498	4.2 ^a		
1.8	1.482	3.2	1.483	1.504
2.2	1.470	4.4	1.471	1.500
2.3	1.471	4.3	1.471	1.501
3.1	1.433	6.6		1.490
3.2	1.430	5.5		1.488
3.7	1.406	9.0		

^aComposed peak.

While x-ray methods alone do not allow the establishment of the actual composition profile, this is possible in combination with photoluminescence (PL) spectroscopy. To obtain PL and PL excitation (PLE) spectra the samples were kept at 8 K in an optical flow-through cryostat cooled by liquid helium. Excitation of the spectra was by a tunable Ti-sapphire laser pumped by an Ar⁺ laser. Luminescence spectra were excited by the above-bandgap-light $\lambda = 800$ nm. Excitation power for the spectra presented in this paper was ~ 20 mW/mm². Signals were analyzed by a 1-m double monochromator set in all cases to a resolution better than 0.5 meV, and detected by a cooled photomultiplier with GaAs photocathode, using photon counting techniques. The sharpness of the In compositional profile is known to be related to the energy of the heavy-hole to electron transition.^{13,16} From the analysis of optical data we deduced that In segregation in our samples is suppressed in comparison to previous reports, both for (100) and (311)*A* orientations.¹⁴ We shall return to this point at a later time.

III. STRUCTURAL CHARACTERIZATION BY X-RAY DIFFRACTION

HRDXD studies of ultrathin, strained InAs films have been carried out previously for the case of (100)-oriented layers with a thickness of around or larger than one monolayer.⁹ We therefore do not present the complete set of HRDXD data but concentrate on two illustrative and representative samples.

Figures 1(a) and 1(b) show the HRDXD spectra of the first sample with a nominal InAs thickness of 0.4 \AA . These spectra demonstrate the sensitivity of HRDXD to very small amounts of strained material. The theoretical simulations of the (311) and (400) spectra, based on the artificial assumption of a 0.4- \AA -thick InAs layer, are also shown in Figs. 1(a) and 1(b). The close similarity between simulations and experimental results shows that this InAs structure with its far from complete coverage of the (311)-lattice plane already behaves like a quantum-well structure in these HRDXD experiments. This obser-

vation is also made for all other investigated samples that give rise to comparable spectra that evolve continuously with InAs thickness.

Figures 2(a) and 2(b) give the HRDXD spectra of a (311) sample with a much larger InAs thickness of 3.2 Å. Again the theoretical simulation reproduces the experimental results very well. It is noticeable, however, that for the (400) reflection we find a much better agreement between theory and experiment if we require the InAs unit cell to exhibit a shear strain component according to the equations derived by De Caro and Tapfer.¹⁷ Earlier approximated theories for the strain state of such layers^{18,19} give a vanishing shear strain component which leads to significant discrepancies between theoretical and experimental results. This fact is illustrated in Fig. 2(b) where the simulation assuming zero shear strain clearly departs from the experimental HRDXD pattern in the vicinity of the substrate peak. Although a more accurate study of strained (311) layers has to be carried out using structures optimized for such a measurement, i.e., (311)-InAs/GaAs superlattice samples, these results indicate the presence of shear strain in these samples. We therefore calculate the strains after De Caro and Tapfer¹⁷ for the band structure calculations presented in Sec. V.

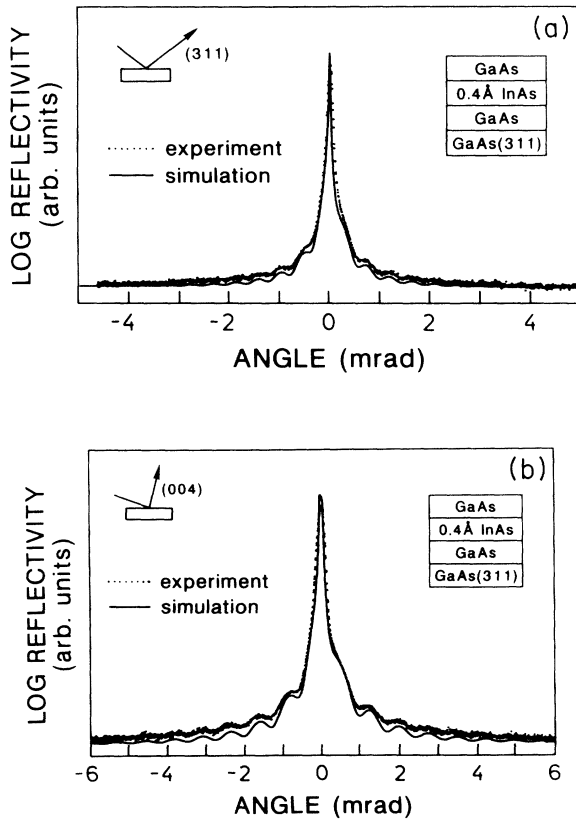


FIG. 1. High-resolution x-ray diffraction patterns of a 0.4-Å (311) InAs film taken in the vicinity of (a) the symmetrical (311) and (b) the asymmetrical (004) reflection. Points are experimental data, lines are the results of theoretical simulations.

IV. RESULTS OF OPTICAL MEASUREMENTS

In this section, we discuss the general features of PL and PLE spectra, which are similar for (100)- and (311)-oriented samples. For the following discussion we neglect the influence of piezoelectric fields on the spectra of (311)-oriented samples. We have observed only insignificant shifts of less than 1 meV in the position of the PL peaks with change in excitation density. This observation conforms with the theoretical expectation¹⁸ of a potential step of only 3 meV across the InAs well.

In contrast to the HRDXD measurements, the optical measurements indicate that our set of samples splits up in two different groups. Above an InAs thickness of 1.8 Å the samples exhibit PL and PLE spectra with well-defined peaks characteristic of a quantum-well structure. Figure 3 shows typical spectra for such samples. The PL spectra consist of a single narrow peak related to the

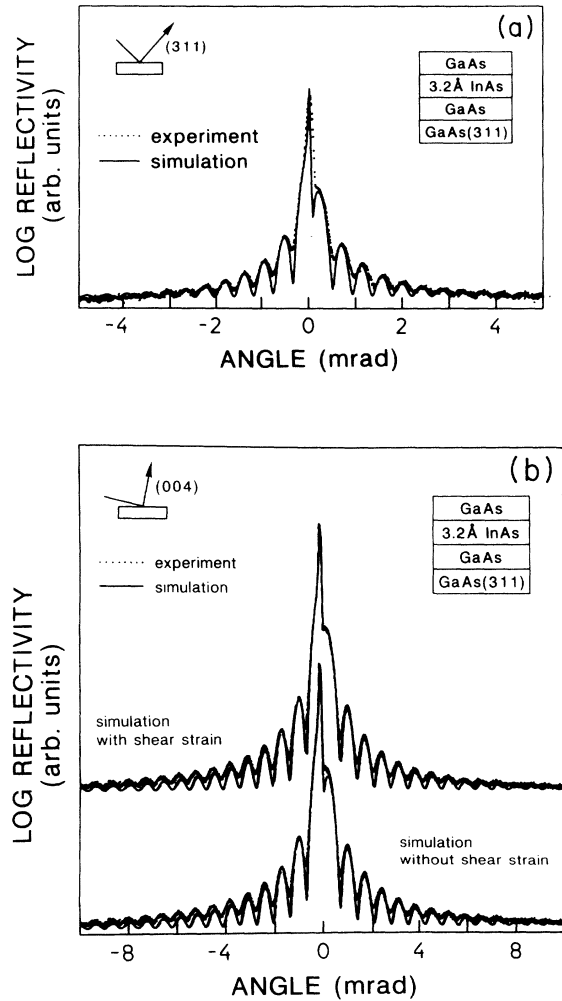


FIG. 2. Simulated and experimental x-ray diffraction pattern of a 3.2-Å InAs film. (a) Symmetrical reflection. (b) Asymmetrical reflection. In this case we compare simulations assuming vanishing and nonvanishing shear strain components.

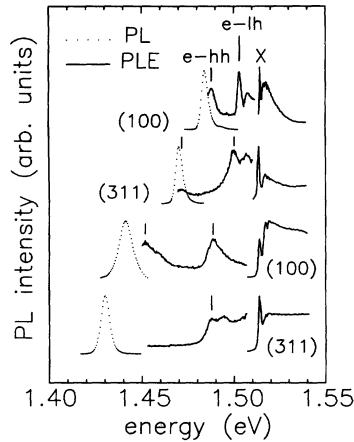


FIG. 3. Comparison of PL and PLE spectra of pairs of samples grown side by side on differently oriented substrates. The orientations are indicated beside each curve, and the In contents are as follows: $d_{\text{InAs}} = 2.0 \text{ \AA}$ (curve A), $d_{\text{InAs}} = 2.3 \text{ \AA}$ (curve B), $d_{\text{InAs}} = 3.2 \text{ \AA}$ (curve C), $d_{\text{InAs}} = 3.2 \text{ \AA}$ (curve D).

InAs layer. The energy position and full width at half maximum (FWHM) of this peak depend both on d_{InAs} and the sample orientation. Both quantities are listed in Tables I and II for (100)- and (311)-oriented samples, respectively. The PLE spectra are dominated by two peaks or groups of peaks around the heavy-hole to electron (e -hh) and light-hole to electron (e -lh) transitions. These assignments have been demonstrated in (100)-oriented samples by modulated reflectance techniques²⁰ and by polarization-dependent measurements.²¹ From the similarity of the spectra we tentatively assign the high-energy feature observed in PLE spectra of (311)-oriented samples to the e -lh transition. These transition energies are independent of detection energy and are summarized in Tables I and II.

Samples with InAs layers thinner than $\sim 1.8 \text{ \AA}$ deviate from the familiar quantum-well behavior and may be better described as an array of two-dimensional InAs clusters. A first hint for this nonstandard behavior comes from excitation-density-dependent PL experiments. Figure 4 displays two PL spectra of the 1.1-\AA (100) sample excited with two different power densities. The band around 1.495 eV is identified as carbon-related transitions in GaAs and, accordingly, its intensity saturates when the excitation density is increased. The other two peaks observed at 1.508 eV and 1.515 eV increase in intensity for higher excitation. The former is ascribed to the insertion of an InAs submonolayer into the GaAs matrix, whereas the latter corresponds to the free-exciton transition in GaAs. From the change in the intensity ratio between InAs-related and free-exciton GaAs peaks it is obvious that even at this comparatively low excitation density of 200 mW/mm^2 the InAs-related peak tends to saturate. This is in striking contrast to the behavior of thicker InAs layers which show a strictly linear dependence of the PL intensity up to excitation densities of 10^3 mW/mm^2 . Similarly, the PLE spectra of the thinnest samples clearly deviate from the observations made for thicker samples. The PLE spectrum of the 1.1-\AA

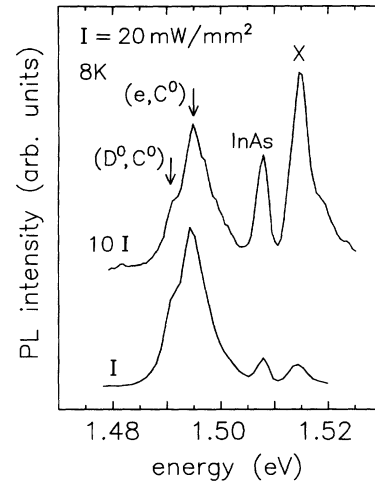


FIG. 4. Photoluminescence spectra of the (100)-oriented sample with $d_{\text{InAs}} = 1.1 \text{ \AA}$ taken at two different excitation densities.

\AA (100) sample displayed in Fig. 5, for example, shows an abnormally negative Stokes shift whereas the thicker samples all exhibit the familiar behavior of a PL peak Stokes shifted to lower energies. The PLE spectra of the corresponding (311) sample are equivalent and omitted for space reasons. The next (100) sample, whose PLE spectrum is displayed in Fig. 6, exhibits a broad absorption band starting at 1.510 eV from which a sharp peak rises at 1.502 eV . This PLE spectrum is clearly not the spectrum of a quantum-well structure although the x-ray spectra show no difference between this and other samples. The PL peak of the corresponding (311) sample occurs almost at the position of the carbon band and a reasonable PLE spectrum can only be taken by detecting on the far high-energy side of the PL peak. Consequently the information contained in it is incomplete, but as shown in Fig. 7 we observe a broad absorption band, as in the (100) sample.

These unusual features can be understood by considering the microscopic structure of our submonolayer InAs samples. The presence of a $\text{Ga}_x\text{In}_{1-x}\text{As}$ alloy layer with appropriate composition cannot explain all experimen-

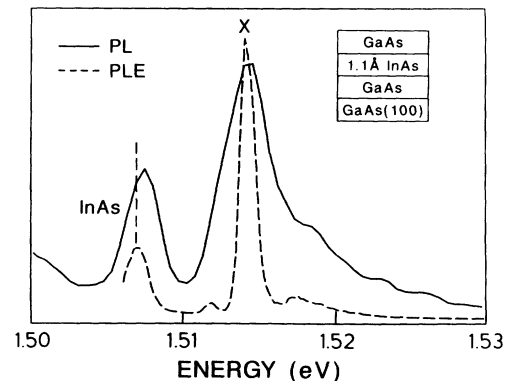


FIG. 5. Photoluminescence excitation spectrum of the 1.1 \AA (100) sample. Note the anomalously negative Stokes shift.

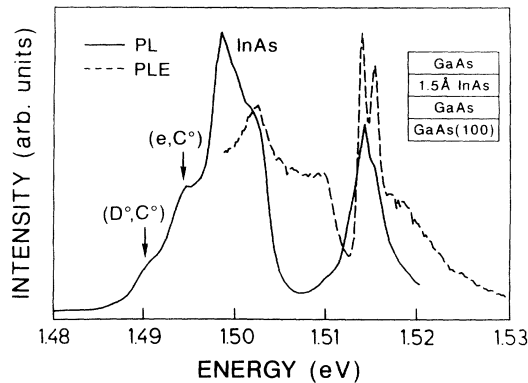


FIG. 6. Photoluminescence excitation spectrum of the 1.5-Å-thick (100)-oriented sample.

tal facts. It is clear that on going from monolayer to submonolayer coverages the initially coherent InAs film becomes more and more punctured by GaAs intrusions. It is important to know the length scale on which these intrusions occur. The shift in PL energy requires that the lateral extent of InAs islands and their separation are much smaller than the exciton size,²² thus in the range of a few Å up to 10 nm. The existence of an InAs island or cluster structure implies that the lateral transport of excitons can be partially or completely suppressed by the GaAs intrusions. And indeed, time-resolved measurements²³ show a spectral blueshift with time in our thinnest samples in accordance with the observations in InAs quantum dot structures prepared on vicinal GaAs substrates.²⁴ In the thicker samples, as the suppression of the lateral diffusion is gradually relaxed, this behavior gives way to a spectral redshift. The existence of a lateral localization can account for the observed negative Stokes shift. Since no lateral carrier diffusion can occur, the PLE measurement only contains information about one specific InAs cluster size. The PLE maximum then occurs at the energy characteristic for this particular size. The PL signal, however, peaks at a different point which is a complex function of the cluster size distribution, the capture and radiative efficiency of the individual clusters. Therefore the PL peak

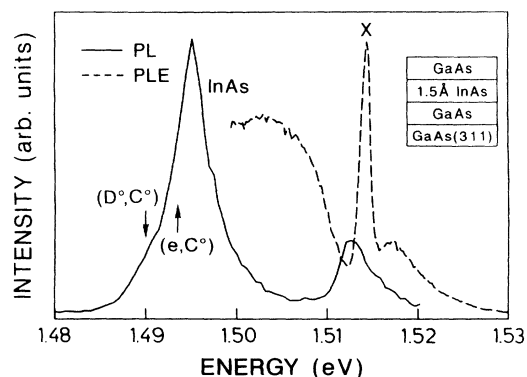


FIG. 7. Photoluminescence excitation spectrum of the 1.5-Å-thick (311)-oriented sample.

could very well occur at an energy *higher* than the PLE maximum and we are thus left with a negative Stokes shift. For the slightly thicker 1.5-Å samples PLE reveals a broad absorption band indicating a fluctuating cluster size. But in these structures the lateral transport is already operational and therefore the narrow PL signal stems exclusively from the low-energy end of this absorption band. These observations bring us to the important conclusion that a quantum-well model can be applied to these ultrathin InAs films starting from thicknesses between 1.5 and 2 Å. This finding is valid for (100)- and for (311)-oriented samples.

V. CALCULATION AND DISCUSSION

In order to study the variation of electronic transition energies with InAs layer thickness and the differences between (100) and (311) orientations we have performed calculations using an eight-band $\mathbf{k} \cdot \mathbf{p}$ -type model. In this model, the InAs layer is treated as a square potential well whose thickness is a continuously variable parameter. This model is consistent with the limiting case of an isoelectronic In impurity in GaAs. The insertion of an In atom in GaAs causes a local band gap reduction of the host GaAs crystal rather than inducing a distinct impurity level in the GaAs gap.²⁵

The band structure of the bulk constituents is described by an $8 \times 8 \mathbf{k} \cdot \mathbf{p}$ matrix including stress terms and spin-orbit interaction,²⁶ so that band mixing effects, non-parabolicity, and band anisotropy are taken into account in a natural way. This model is therefore well suited to perform a comparative study of transition energies in samples with different thickness and orientation. For the calculation we use accepted values of effective masses of GaAs and InAs and their band gaps at low temperature (see Table III). For the (311) orientation we have considered different values of the effective masses of the heavy holes in [111] direction of both constituents. We shall discuss the influence of these effective masses later on. The appropriate strain tensor for each orientation is obtained from elasticity theory¹⁷ using tabulated values²⁷ of the elastic stiffness constants. The energies of the strained band edges at Γ of bulk InAs are calculated using the following deformation potentials:²⁷ $a = -5.8$ eV, $b = -1.8$ eV, and $d = -3.6$ eV, where a is the hydrostatic deformation potential and b and d describe the hh-lh splitting under [100] and [111] stress, respectively.

The fractional conduction-band (CB) offset, $Q_C = \Delta E_C / \Delta E_G$, where ΔE_G is the difference in the (stressed) heavy-hole band gap and ΔE_C is the CB discontinuity, entered as a parameter in the calculation. Instead of leaving Q_C as a fitting parameter, we rely on values

TABLE III. Different parameters used in the calculations.

Compound	m_e^*	m_{hh}^*	m_{lh}^*	$m_{s.o.}^*$	E_g (eV)	$\Delta_{s.o.}$ (eV)
GaAs	0.0665	0.377	0.0905	0.1757	1.519	0.341
InAs	0.0234	0.263	0.0270	0.0836	0.420	0.380

found from the equations given by Van de Walle,²⁸ since this procedure deals with strained-layer interfaces and gives results in good agreement with our measurements, as shown below.

A. Transition energies

Experimental and calculated transition energies are compared in Fig. 8. Figure 8(a) shows results for (100) orientation. The e -hh transition energies as a function of d_{InAs} are remarkably well described by the calculated curve using $Q_C = 0.53$ ($\Delta E_C = 526$ meV), found following Ref. 28. The largest discrepancy occurs with the e -lh transition, where the calculation overestimates the measured energy.

One possible reason for the discrepancy is that In segregation, although small in these samples, is certainly present.²⁹ We have calculated for segregated profiles considering different values of Q_C but in all cases we find even larger discrepancies than that shown in Fig. 8(a). Variation of the calculation parameters, e.g., taking a heavier effective mass for the light holes, does not lead to the expected reduction of the calculated e -lh transition energy, as a result of the interaction of the lh and the spin-orbit-split hole bands. We also made calculations with different values of deformation potentials. At first sight it seems that it is possible to fit both the energy position of the hh and the hh-lh splitting by choosing suitable values of the a and b deformation potentials. Again, for these specific samples, the interplay of different contributions in the calculation does not improve the agreement.

The only way we have found to draw together experiment and theory is to assume that InAs is slightly less strained than expected from elastic theory, yet considering no segregation. That is, the only change in the

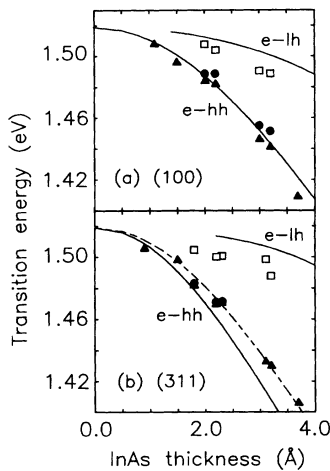


FIG. 8. Energies of the interband electronic transitions as a function of d_{InAs} . Measured PL energies are indicated by triangles, PLE peaks are given by circles (e -hh transitions) and squares (e -lh transitions). Calculated energies are displayed by lines (see text). (a) (100) orientation, (b) (311) orientation.

calculation is to reduce the lattice deformation perpendicular to the growth plane, ϵ_{zz} . In this way, the discrepancy is reduced because strain affects the hh and lh levels differently. It is obvious that to obtain a good fit of both the e -hh and e -lh transition energies using a reduced strain configuration for the InAs layer, it is also necessary to modify the value of ΔE_C , but Q_C remains almost unchanged due to the always concomitant change in ΔE_G . For example, taking the 2-Å-thick (100) sample, we obtain a satisfactory agreement with experiment by using $\epsilon_{zz} = 0.065$ and $\Delta E_C = 500$ meV (which in this case corresponds to $Q_C = 0.51$). This result is consistent both with the idea of having InAs islands of reduced lateral dimensions,³⁰ and with a possible breakdown of continuum elasticity theory for monolayer films.³¹ In any case, we obtain CB offset ratios Q_C around 0.5 for the strained interface InAs/GaAs (100).³² The value of band offset for the strained interfaces $\text{Ga}_{1-x}\text{In}_x\text{As}/\text{GaAs}$ (100) is controversial.³³ For $x = 1$, Hirakawa *et al.*³⁴ have determined ΔE_C by x-ray photoelectron spectroscopy to be 0.38 eV. They discuss the crucial dependence of this value upon the strain state of the layer. A reduction in this strain state would change this energy offset towards the unstrained value 0.9 eV.³⁵ For our particular samples, the offset value calculated according to van de Walle²⁸ explains our results satisfactorily. Our main conclusions stem from the comparison of results of the dependence on d_{InAs} and sample orientation, which are invariant for Q_C near 0.5.

Figure 8(b) compares the transition energies measured and calculated in (311) samples. The weak thickness dependence of the high-energy feature observed in the PLE spectra confirms the previous assignment of the e -lh transition. The lh level is unbound for InAs thicknesses smaller than 2.2 Å. Again, a slight reduction of strain in InAs is needed to bring this calculated energy closer to experiment.

The e -hh transitions in our (311)-oriented structures always appear at lower energies than in their (100)-oriented counterparts, in contrast to the report by Meléndez *et al.*¹³ This result implies the low In segregation exhibited by our (311) samples. There are two contributions to this observed difference; the intrinsic valence-band anisotropy of the bulk constituents, already observed in lattice matched $\text{GaAs-Al}_x\text{Ga}_{1-x}\text{As}$ structures,³⁶⁻³⁸ and the anisotropy effect induced by the strain. The added contributions give the total observed anisotropy.

In Fig. 8(b), solid lines correspond to the calculation using $Q_C = 0.44$ ($\Delta E_C = 431$ meV). The band offset ratio found²⁸ in this case is smaller than in (100) orientation due to the difference in hydrostatic deformations of the biaxially strained InAs lattice. The dashed line corresponds to the e -hh transition energy calculated with the same Q_C as in the (100) case, but taking into account the stressed hh band gap of InAs, resulting in $\Delta E_C = 517$ meV. In the latter case, we obtain no bound lh level. These curves are calculated for $m_{\text{hh},(111)}^* = 1$ (Ref. 39) for both constituents. Naturally, if we take a smaller mass anisotropy either for GaAs or InAs, or both, the calculated energies become larger. For example, the

dashed line in Fig. 4(b) can also be obtained by taking $m_{(111),\text{GaAs}}^* = 0.7$ (Ref. 37) and $Q_C = 0.44$. Both the effect of valence-band anisotropy and strain-dependent band offset are responsible for the observed differences, although from the present data we cannot unequivocally separate both contributions, mainly because the mass anisotropy is not a well established quantity. Bearing in mind that the enhanced segregation in (311) orientation with respect to (100) orientation⁴⁰ reduces the observed anisotropy relative to its “true” value, we conclude that, for the accepted values of valence-band anisotropy, our data require a direction-dependent band offset, in agreement with the model-solid theory.²⁸

B. Photoluminescence linewidth

The linewidth of the PL lines is found to increase with d_{InAs} and is systematically smaller for (311) than for (100) samples. These correlated linewidth differences are predominantly caused by fluctuations in the recombination energy of the excitons given in turn by local fluctuations of d_{InAs} . Singh and Bajaj⁴¹ have studied the linewidth broadening in PL of quantum-well structures produced by interface roughness and alloy disorder. In the present case, the role of alloy disorder, assuming that In segregation leads to some alloying, must be smaller than the linewidth due to roughness. Otherwise, we would expect PL emission from (311) samples to be broader, because they display an enhanced In segregation and also the slope of the energy as a function of d_{InAs} is larger for this orientation. This means that fluctuations in the scale length of the exciton are smaller for (311) than for (100) samples. This is consistent also with the smaller Stokes shifts found in (311) samples.

In order to somewhat quantify the ideas revealed above, we follow the lines of Ref. 41. Knowing the dependence on d_{InAs} of the PL energy and the experimental linewidths, we can estimate the average roughness of the InAs film. Taking for the exciton diameter the value in bulk GaAs, we find a lateral extension of InAs islands of $\sim 10\text{\AA}$ for all the (311) samples, their difference in FWHM being given solely by the energy slope. In (100) samples, the values found scatter around 15\AA , up to 30\AA for the thickest sample. We regard these values as qualitative estimates but indicative of the microscopic structure of the samples. Noda *et al.*⁶ deduced from their electrical measurements on a 1.6-\AA -thick (100) InAs film a correlation length of the InAs islands of 13 nm . However, the growth method employed in their work is slightly different from ours and therefore a substantial variation of this value cannot be excluded. In our case the observed Stokes shifts also indicate that the roughness pattern is more regular in (311)-oriented samples than in (100) orientation. Since no indication of lateral

patterning effects due to surface corrugation⁴² has been found in InAs/GaAs (311), we believe that our observations show that processes occurring during strained layer growth such as terrace nucleation and coherent islanding are different on (100) and (311) surfaces and imply that the roughness of these films and shape of the resulting InAs islands is very different in spite of the RHEED pattern being two dimensional in both cases.

VI. CONCLUSIONS

We have reported results obtained in ultrathin InAs layers embedded within GaAs. The optical study as a function of In content for two different crystal orientations has served to gain some insight into their structural and electronic properties.

From the structural point of view we find that the samples exhibit very sharp InAs distribution profiles. Several results indicate that InAs is arranged in islands of lateral sizes of the order of 10\AA , rather than forming a homogeneous GaInAs alloy. Optical spectroscopy reveals a clear crossover from electronically disconnected clusters to quantum-well behavior at an InAs density of $3 \times 10^{14}\text{ cm}^{-2}$ for both (100) and (311) orientations.

The dependence upon In content of the InAs-related electronic transitions observed in the quantum-well-like (100)-oriented samples is well explained by an eight-band $\mathbf{k} \cdot \mathbf{p}$ envelope-function calculation without any fitted parameters, where the band offset ratio is taken from calculations using the model-solid theory.²⁸ Transition energies in the (311)-oriented samples differ from the (100) case due to intrinsic anisotropy effects. The added effects of valence-band anisotropy and of strain-induced anisotropy of the band offset give the total observed differences. Although we cannot separate these two contributions experimentally, by using the known valence-band anisotropies, we find that the change in band offset is of the order of magnitude given by van de Walle.²⁸ Thus it becomes clear from this study that in strained interfaces the band lineups depend on microscopic details of the interface, such as orientation.

ACKNOWLEDGMENTS

We would like to thank M. Garriga, R. Nötzel, and E. Tournié for helpful and encouraging discussions, A. Fischer for valuable help in molecular-beam epitaxy growth, A. Lehmann for help with the optical setup, and C. Whitaker for a careful reading of the manuscript. One of the authors, M.I.A., is grateful to the Paul-Drude-Institut for financial support. Part of this work was sponsored by the Bundesministerium für Forschung und Technologie of the Federal Republic of Germany.

¹ N. Grandjean, J. Massies, and V. H. Etgens, Phys. Rev. Lett. **69**, 796 (1992).

² H. Presting, H. Kibbel, M. Jaros, R. M. Turton, U. Menciagar, G. Abstreiter, and H. G. Grimmeis, Semicond. Sci.

Technol. **7**, 1127 (1992).

³ H. Morkoç, B. Sverdlov, and B. G. Gao, IEEE Proc. (to be published).

⁴ K. J. Moore, G. Duggan, K. Woodbridge, and C. Roberts,

- Phys. Rev. B **41**, 1090 (1990).
- ⁵ Y. Matsui, H. Hayashi, and K. Yoshida, Appl. Phys. Lett. **48**, 1060 (1986).
- ⁶ T. Noda, M. R. Fahy, T. Matsusue, and H. Sakaki, J. Cryst. Growth **127**, 783 (1993).
- ⁷ F. J. Grunthaler, M. Y. Yen, R. Fernandez, T. C. Lee, A. Madhukar, and B. F. Lewis, Appl. Phys. Lett. **46**, 983 (1985).
- ⁸ M. A. Tischler, N. G. Anderson, and S. M. Bedair, Appl. Phys. Lett. **49**, 1199 (1986).
- ⁹ O. Brandt, L. Tapfer, R. Cingolani, K. Ploog, M. Hohenstein, and F. Philipp, Phys. Rev. B **41**, 12 599 (1990).
- ¹⁰ D. S. McCallum, X. R. Huang, T. F. Boggess, M. D. Dawson, A. L. Smirl, and T. C. Hasenberg, J. Appl. Phys. **69**, 3242 (1991).
- ¹¹ S. S. Dosanjh, P. Dawson, M. R. Fahy, B. A. Joyce, R. Murray, H. Toyoshima, X. M. Zhang, and R. A. Stradling, J. Appl. Phys. **71**, 1242 (1992).
- ¹² M. Ilg and K. H. Ploog, Appl. Phys. Lett. **62**, 997 (1993).
- ¹³ J. Meléndez, A. Mazuelas, P. S. Dominguez, M. Garriga, M. I. Alonso, G. Armelles, L. Tapfer, and F. Briones, Appl. Phys. Lett. **62**, 1000 (1993).
- ¹⁴ M. Ilg, M. I. Alonso, A. Lehmann, K. H. Ploog, and M. Hohenstein, J. Appl. Phys. **74**, 7188 (1993).
- ¹⁵ L. Tapfer, M. Ospelt, and H. von Känel, J. Appl. Phys. **61**, 1298 (1990).
- ¹⁶ M. Sato and Y. Horikoshi, J. Appl. Phys. **69**, 7697 (1991).
- ¹⁷ L. De Caro and L. Tapfer, Phys. Rev. B **48**, 2298 (1993).
- ¹⁸ D. L. Smith and C. Mailhot, J. Appl. Phys. **63**, 2717 (1988).
- ¹⁹ E. A. Caridi and J. B. Stark, Appl. Phys. Lett. **60**, 1441 (1992).
- ²⁰ P. Castrillo, G. Armelles, A. Ruiz, and F. Briones, Jpn. J. Appl. Phys. **30**, L1784 (1991).
- ²¹ O. Brandt, H. Lage, and K. Ploog, Phys. Rev. B **45**, 4217 (1992).
- ²² K. Taira, H. Kawai, I. Hase, K. Kaneko, and N. Watanabe, Appl. Phys. Lett. **53**, 495 (1988).
- ²³ M. Ilg and K. H. Ploog (unpublished).
- ²⁴ O. Brandt, L. Tapfer, K. Ploog, R. Bierwolf, M. Hohenstein, F. Philipp, H. Lage, and A. Heberle, Phys. Rev. B **44**, 8043 (1991).
- ²⁵ W. Czaja, in *Festkörperprobleme (Advances in Solid State Physics)*, edited by O. Madelung (Vieweg, Braunschweig, 1971), Vol. 11, p. 65.
- ²⁶ M. F. H. Schuurmans and G. W. 't Hooft, Phys. Rev. B **31**, 8041 (1982).
- ²⁷ *Landolt Börnstein: Numerical Data and Functional Relationships in Science and Technology*, edited by O. Madelung (Springer, Berlin, 1982), Vol. 17a.
- ²⁸ C. G. Van de Walle, Phys. Rev. B **39**, 1871 (1989).
- ²⁹ C. Giannini, L. Tapfer, S. Lagomarsino, J. C. Boulliard, A. Taccoen, B. Capelle, M. Ilg, O. Brandt, and K. H. Ploog, Phys. Rev. B **48**, 11 496 (1993).
- ³⁰ J. Massies and N. Grandjean, Phys. Rev. Lett. **71**, 1411 (1993).
- ³¹ O. Brandt, K. Ploog, R. Bierwolf, and M. Hohenstein, Phys. Rev. Lett. **68**, 1339 (1992).
- ³² The value obtained in Ref. 14 is underestimated due to the fit made considering the InAs submonolayers as one-monolayer-thick $\text{Ga}_x\text{In}_{1-x}\text{As}$ alloys of appropriate composition, while taking E_G as a fit parameter.
- ³³ See, for instance, M. J. Joyce, M. J. Johnson, M. Gal, and B. F. Usher, Phys. Rev. B **38**, 10 778 (1988), and references cited therein.
- ³⁴ K. Hirakawa, Y. Hashimoto, K. Harada, and T. Ikoma, Phys. Rev. B **44**, 1734 (1991).
- ³⁵ S. P. Kowalczyk, W. J. Schaffer, E. A. Kraut, and R. W. Grant, J. Vac. Sci. Technol. **20**, 705 (1982).
- ³⁶ T. Hayakawa, K. Takahashi, M. Kondo, T. Suyama, S. Yamamoto, and T. Hijikata, Phys. Rev. Lett. **60**, 349 (1988).
- ³⁷ L. W. Molenkamp, R. Eppenga, G. W. 't Hooft, P. Dawson, C. T. Foxon, and K. J. Moore, Phys. Rev. B **38**, 4314 (1988).
- ³⁸ D. Gershoni, I. Brener, G. A. Baraff, S. N. G. Chu, L. N. Pfeiffer, and K. West, Phys. Rev. B **44**, 1930 (1991).
- ³⁹ This value results in $m_{\text{hh},(311)}^* \approx 1.5 m_{\text{hh},(100)}^*$ for both bulk constituents, as given by J. B. Xia, Phys. Rev. B **43**, 9856 (1991).
- ⁴⁰ M. Ilg and K. H. Ploog, Phys. Rev. B **48**, 11 512 (1993).
- ⁴¹ J. Singh and K. K. Bajaj, J. Appl. Phys. **57**, 5433 (1985).
- ⁴² M. Ilg, R. Nötzel, K. H. Ploog, and M. Hohenstein, Appl. Phys. Lett. **62**, 1472 (1993).